

# Optimal Frames for Polarisation State Reconstruction

Matthew R. Foreman<sup>1,\*</sup>, Alberto Favaro<sup>2</sup>, and Andrea Aiello<sup>1</sup>

<sup>1</sup>*Max Planck Institute for the Science of Light, Günther-Scharowsky-Straße 1, 91058 Erlangen, Germany*

<sup>2</sup>*Blackett Laboratory, Department of Physics, Imperial College London, Prince Consort Road, London, SW7 2AZ, UK*

Complete determination of the polarisation state of light requires at least four distinct projective measurements of the associated Stokes vector. Stability of state reconstruction, however, hinges on the condition number  $\kappa$  of the corresponding instrument matrix. Optimisation of redundant measurement frames with an arbitrary number of analysis states,  $m$ , is considered in this Letter in the sense of minimisation of  $\kappa$ . The minimum achievable  $\kappa$  is analytically found and shown to be independent of  $m$ , except for  $m = 5$  where this minimum is unachievable. Distribution of the optimal analysis states over the Poincaré sphere is found to be described by spherical 2-designs, including the Platonic solids as special cases. Higher order polarisation properties also play a key role in nonlinear, stochastic and quantum processes. Optimal measurement schemes for nonlinear measurands of degree  $t$  are hence also considered and found to correspond to spherical  $2t$ -designs, thereby constituting a generalisation of the concept of mutually unbiased bases.

PACS numbers: 42.25.Ja, 03.65.Wj, 07.60.Fs, 02.40.-k, 02.10.Ud, 42.50.Dv

Measurement of the polarisation of light is a common problem in many fields of physics including quantum information, astronomy, quantitative biology and single molecule orientational imaging [1–4]. Typically, determination of the polarisation state of light, as parameterised by a  $4 \times 1$  Stokes vector,  $\mathbf{S}$ , follows by making projective measurements onto a set of known analysis states, with complete state reconstruction requiring a minimum of four distinct measurements [5]. Arguably the simplest so-called complete polarimeter is that which comprises of linear polarisers, oriented at  $0^\circ$ ,  $45^\circ$  and  $90^\circ$  to some reference axis, and a circular polariser. By virtue of the linear nature of the measurement process, the intensities transmitted through each polarisation state analyser (PSA), denoted by  $\mathbf{D}$ , can be related to the incident Stokes vector via  $\mathbf{D} = \mathbf{A}\mathbf{S}$ , where  $\mathbf{A}$  is known as the instrument matrix (in this example  $\mathbf{D}$  is  $4 \times 1$  and  $\mathbf{A}$  is  $4 \times 4$  in dimension). Although intuitively simple to understand and easy to implement, this polarimeter performs sub-optimally. Much effort has been invested over the years to optimise the geometry of polarimeters using metrics such as the total variance on the inferred Stokes vector [6, 7], information content [8–11], the determinant of the instrument matrix [12–14] and signal to noise ratio [15]. Perhaps most popular, however, is the condition number,  $\kappa$ , of the instrument matrix [13–20] which describes the stability of the polarisation inference problem regardless of reconstruction algorithm and bounds the extent to which relative measurement errors are amplified during state reconstruction. Smaller condition numbers imply more robust measurements. Use of a measurement set of greater than four analysis states, however, is known to mitigate the effects of noise [8, 20, 21]. Nevertheless, only limited consideration has been given to optimisation of these systems. Drawing from results in discrete computational geometry, linear algebra and state tomography this work hence considers the optimisation of such

measurement schemes in the sense of minimisation of  $\kappa$  and discusses the associated geometric interpretation. It is established analytically that the minimum condition number is  $\sqrt{20}$  independent of the number of analysis states. Formal equivalence between minimisation of  $\kappa$ , maximisation of the determinant of the associated Gram matrix and minimisation of the equally weighted variance is established. Optimality constraints are further derived and used to construct some illustrative optimal measurement sets. More specifically, it is found that the distribution of optimal analysis states over the Poincaré sphere is intimately related to spherical 2-designs. Accordingly, in contrast to previous reports, optimal measurements are shown not to necessarily correspond to inscribed polyhedra of maximal volume.

Going beyond linear reconstruction of the Stokes vector, measurements of more complex functions of the Stokes vector,  $D(\mathbf{S})$ , are made in a number of applications. Nonlinear light scattering and material characterisation, for example, gives rise to intensities which depend on products of Stokes parameters [22, 23]. Furthermore, random media and rough surfaces can be studied through the changes in the statistical properties of the polarisation of light induced upon transmission or reflection [24–26]. Full characterisation, however, requires determination of the underlying probability distribution function, or equivalently all higher order statistical moments of the Stokes parameters. Optimal analysis states for such higher order problems are also considered in this Letter and their relationship with spherical  $t$ -designs established. Importantly, although the language of classical polarimetry will be used throughout, it should be noted that the results given are equally applicable in the quantum regime for states of a given number of photons. For example, knowledge of higher order moments of the Stokes operators can give insight into hidden “quantum” polarisation in a classically unpolarised state [27, 28].

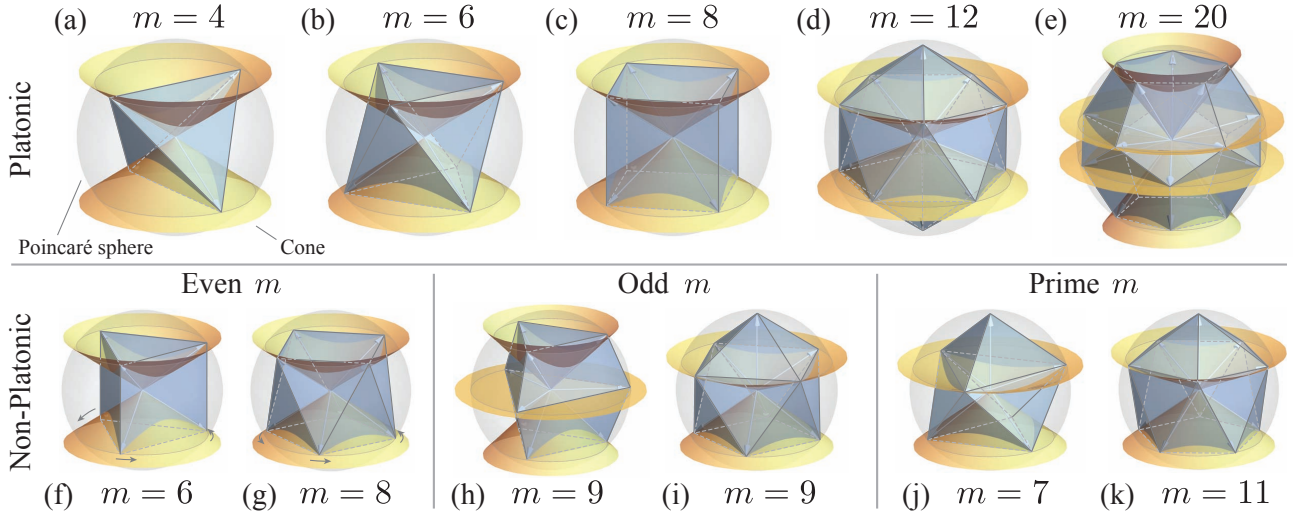


FIG. 1: (a)-(e) Optimal measurement frames for  $m = 4, 6, 8, 12$  and  $20$  defining the Platonic polyhedra inscribed in the Poincaré sphere. Corresponding analysis states lie on the family of cones shown. (f)-(k) Example optimal measurement frames and associated non-Platonic polyhedra for  $m = 6, 8, 9, 7$  and  $11$ .

The action of a PSA on incident light of arbitrary polarisation, can be considered as a projective measurement, whereby the output light has polarisation matching the nominal analysis state of the PSA (denoted  $\mathbf{A} = (1, A_1, A_2, A_3)^T/2$  with  $\sum_{k=1}^3 A_k^2 = 1$ ) and intensity of  $\mathbf{A}^T \cdot \mathbf{S}$ , where  $\mathbf{A}$  has been normalised to ensure the PSA is passive [9]. Each row of the instrument matrix associated with  $m \geq 4$  different measurements is given by  $\mathbf{A}_j$  ( $j = 1, 2, \dots, m$ ) and  $\mathbb{A}$  thus has dimension  $m \times 4$ . The corresponding vector of measured intensities,  $\mathbf{D}$ , is hence  $m \times 1$ . Geometrically, each  $\mathbf{A}_j$  can be considered as defining a point on the surface of the Poincaré sphere through the reduced vector  $\mathbf{a}_j = (A_{j1}, A_{j2}, A_{j3})^T$ , such that  $\mathbb{A}$  defines the vertices of a polyhedron inscribed within the unit sphere. Moreover, the set of vectors  $\{\mathbf{a}_j\}$  constitutes a measurement frame [15].

The condition number of the instrument matrix is explicitly defined as  $\kappa = \|\mathbb{A}\| \|\mathbb{A}^+\|$ , where  $\mathbb{A}^+$  denotes the generalised inverse of  $\mathbb{A}$  and  $\|\cdot\|$  denotes the matrix norm (taken as the Hilbert-Schmidt norm throughout this work). Noting that the normalisation imposed on the rows of  $\mathbb{A}$  requires  $\mathbf{A}_j^T \cdot \mathbf{A}_j = 1/2$ , it follows that

$$\|\mathbb{A}\|^2 = \text{tr}[\mathbb{A}^T \mathbb{A}] = m/2. \quad (1)$$

For any given experimental setup  $\|\mathbb{A}\|$  is thus constant. Accordingly, minimisation of the condition number is equivalent to minimisation of  $\|\mathbb{A}^+\|^2$ , an alternative figure of merit known as the equally weighted variance (EWV) [6, 20]. The EWV quantifies the noise amplification in the reconstructed Stokes vectors assuming a least norm reconstruction and equal magnitude errors on each measurement [6]. Similarly to above  $\|\mathbb{A}^+\|^2 = \text{tr}[(\mathbb{A}^+)^T \mathbb{A}^+] = \text{tr}[\mathbb{B}^{-1}]$ , where  $\mathbb{B} = \mathbb{A}^T \mathbb{A}$  is a  $4 \times 4$  ma-

trix and  $\mathbb{B}^{-1}$  denotes its inverse. The inverse of  $\mathbb{B}$  exists if  $\mathbf{a}_j$  are not all co-planar and moreover can be written in the form  $\mathbb{B}^{-1} = \text{adj}[\mathbb{B}]/|\mathbb{B}|$  where  $|\cdot|$  and  $\text{adj}[\cdot]$  denote the determinant and adjunct of a matrix respectively. The condition number ( $\kappa > 0$ ) can thus be expressed as

$$\kappa^2 = \text{tr}[\mathbb{B}] \text{tr}[\mathbb{B}^{-1}] = \frac{1}{2} \frac{m}{|\mathbb{B}|} \text{tr} \left[ \frac{d|\mathbb{B}|}{d\mathbb{B}} \right] = \frac{m}{2} \sum_{i=1}^4 \frac{d \ln |\mathbb{B}|}{dB_{ii}} \quad (2)$$

where Jacobi's formula has been used [29] and  $B_{ij}$  is the  $(i, j)$ th element of  $\mathbb{B}$ . Upon differentiation of Eq. (2), application of the product rule and back-substitution it can be shown that  $2 d \ln \kappa = -d \ln |\mathbb{B}|$ . Minimisation of the condition number of the instrument matrix is hence also equivalent to maximisation of the determinant of  $\mathbb{B}$ . Geometrically, it is interesting to note that  $|\mathbb{B}|$  represents the volume squared of a 4-parallelotope in  $\mathcal{R}^m$ . For the special case of  $m = 4$ , maximisation of  $|\mathbb{B}|$  is equivalent to maximising the volume of the tetrahedron whose vertices in  $\mathcal{R}^3$  are defined by  $\mathbf{a}_j$  (see Fig. 1(a)) as has been previously reported [16, 17].

Hadamard's inequality [29] states that the determinant of  $\mathbb{B}$  is upper bounded by the product of its diagonal elements. The maximum determinant is thus obtained when  $\mathbb{B}$  is diagonal whereby the diagonal elements also correspond to the eigenvalues  $\beta_l$  ( $l = 1, \dots, 4$ ). Explicitly  $\mathbb{B}$  can be expressed in the form  $\mathbb{B} = \sum_{j=1}^m \mathbf{A}_j \mathbf{A}_j^T$ , whereby it follows by inspection that  $B_{11} = \beta_1 = m/4$ . Furthermore maximisation of  $|\mathbb{B}|$  is subject to the constraint  $\text{tr}[\mathbb{B}] = m/2$  (c.f. Eq. (1)). Use of the method of Lagrange multipliers then yields  $\beta_1/3 = \beta_2 = \beta_3 = \beta_4 =$

$m/12$ , i.e. the condition number of  $\mathbb{A}$  is minimised when

$$\mathbb{B} = \frac{m}{12} \begin{pmatrix} 3 & 0 & 0 & 0 \\ 0 & 1 & 0 & 0 \\ 0 & 0 & 1 & 0 \\ 0 & 0 & 0 & 1 \end{pmatrix}. \quad (3)$$

Substitution of Eq. (3) into Eq. (2) gives  $\kappa = \sqrt{20} \approx 4.47214$ . The condition number of an optimised polarimeter is hence independent of the number of analysis states  $m$ . It also follows that  $|\mathbb{B}| = m^4/6912$  and the EWV =  $40/m$ . The fall off in the EWV with increasing number of measurements reflects the noise reduction arising from greater measurement redundancy.

Generalisation of the above to the problem of reconstruction of an  $N \geq 3$  dimensional vector  $\mathbf{S}_N = (S_0, S_1, \dots, S_{N-1})^T$ , for which  $S_0^2 \geq \sum_{j=1}^{N-1} S_j^2$ , using  $m \geq N$  projective measurements onto analysis states of the form  $\mathbf{A}_N = (1, A_1, \dots, A_{N-1})^T/2$  can also be easily performed. Consideration of the  $N = 3$  (i.e. reduced dimensionality) case is applicable to linear polarimetry for example, whereas higher dimensional generalisations are relevant to polarimetry of three dimensional fields, whereby Stokes vectors become  $9 \times 1$  in size [26, 30]. Following the steps given above in the  $N$  dimensional case it is found that  $|\mathbb{B}|$  is maximised when  $\mathbb{B}$  is diagonal with non-zero elements of  $\beta_1 = m/4$  and  $\beta_l = \beta_1/(N-1)$  for  $l \neq 1$ . In turn it follows that  $|\mathbb{B}| = (m/4)^N (N-1)^{1-N}$ ,  $\kappa^2 = 2N^2 - 4N + 4$  and the EWV =  $2\kappa^2/m$ .

Whilst the above treatment has considered the minimum achievable condition number and EWV, the optimal measurement basis has not yet been determined. To this end, Eq. (3) must be invoked which upon generalisation implies the set of polynomial constraints

$$\sum_{j=1}^m \mathbf{a}_j = \mathbf{0} \quad \text{and} \quad \sum_{j=1}^m \mathbf{a}_j \mathbf{a}_j^T = \frac{m}{N-1} \mathbb{I}_{N-1}, \quad (4)$$

where  $\mathbb{I}_N$  is the  $N \times N$  identity matrix. A measurement frame is optimal iff Eq. (4) is satisfied. When  $N = 3$  it can be shown [31] that the optimal measurement frame corresponds to  $\mathbf{a}_j$  defining a regular polygon inscribed in a unit circle. Incidentally, the regular inscribed polygons have the maximum area of all inscribed polygons. For the  $N = 4$  case (which is exclusively considered henceforth), it is found that Eq. (4) is satisfied if the set of vectors  $\{\mathbf{a}_j\}$ , or equivalently the vertices of the underlying polyhedron, constitute a spherical 2-design in  $\mathcal{R}^3$  and are thereby closely related to mutually unbiased bases [32]. Proof of this result follows from the definition of spherical  $t$ -designs as a collection of  $m$  points on the surface of the unit sphere in  $\mathcal{R}^3$  for which the (normalised) integral of any polynomial,  $g(\mathbf{S})$ , of degree  $t$  or less is equal to the average taken over the  $m$  points [33, 34]. Use of the polynomial functions  $g = S_j$  and  $S_j S_k$  ( $j$  and  $k = 1, 2, 3$ ) in this definition yields Eq. (4). It is also worthwhile noting that a spherical  $t$ -design is also a  $t-1$  design [33].

Numerical codes can be used for determination of spherical  $t$ -designs in general [35], however, in view of the symmetry of the  $N = 3$  solution, an analogous symmetry in the  $N = 4$  case is expected and can be used to guide the construction of some simple 2-designs. Specifically, letting  $m = rs$ , and adopting the initial ansatz  $\mathbf{a}_j = (\sin \theta_q \cos[\phi_p + \Phi_q], \sin \theta_q \sin[\phi_p + \Phi_q], \cos \theta_q)^T$  for  $j = 1, \dots, m$ ,  $p = 1, \dots, r$ ,  $q = 1, \dots, s$ , where  $\phi_p = 2\pi p/r$ , Eq. (4) reduces to

$$\sum_{q=1}^s \cos \theta_q = 0 \quad \text{and} \quad \sum_{q=1}^s \cos^2 \theta_q = \frac{s}{3}. \quad (5)$$

In general, the solution to Eq. (5), and hence the choice of optimal measurement frame, is not unique (even allowing for the intrinsic rotational freedom). Nevertheless, a number of solutions can be found as is now illustrated.

**Even  $m$ :** For even  $m$  a simple optimal frame follows by taking  $s = 2$  whereby Eq. (5) is trivially satisfied when  $\cos \theta_1 = -\cos \theta_2 = 1/\sqrt{3}$ . Without loss of generality  $\Phi_1$  can also be set to zero. If  $\Phi_2 = 0$  it follows that, depending on the relative sign of  $\sin \theta_1$  and  $\sin \theta_2$ , optimal frames possessing either an inversion or mirror symmetry can be generated. In both cases, however, the vectors  $\mathbf{a}_j$  lie on two cones with apex at the origin and apex angle  $2\theta_q$  (see e.g., Figs. 1(b), (c), (f) and (g) for  $m = 6$  and 8). Geometrically, taking  $\Phi_2 \neq 0$  corresponds to a rotation of the measurement states on the lower cone relative to those on the upper cone as depicted in Figs. 1(f) and (g). Solutions describing the regular tetrahedron  $(m, r, s) = (4, 2, 2)$ , octahedron  $(6, 3, 2)$  and cube  $(8, 4, 2)$  can be generated in this manner (see Figs. 1(a)-(c)).

Going further, a measurement frame containing  $m$  analysis states can be partitioned into  $M$  subsets of size  $m_i = 2\mu_i$ , where  $m = 2 \sum_{i=1}^M \mu_i \equiv 2\mu$ . Optimal bases can then be constructed ( $\Phi_q = 0$  is assumed henceforth for simplicity) by constraining the vectors of each subset to lie on cones with coinciding axes, but with differing apex angles. Explicitly it can then be shown that the apex angles  $\theta_i$  ( $i = 1, \dots, M$ ) of each cone are given by  $\sin^2 \theta_i = 2\mu\lambda_i/(3\mu_i)$ , where  $\sum_{i=1}^M \lambda_i = 1$  [31]. Note that in the limiting case of  $\theta_i \rightarrow 0$  (whereby necessarily  $\mu_i = 1$ ), the corresponding cone collapses to its axis (e.g. Fig. 1(d)). Both the regular icosahedron and dodecahedron can hence be constructed (Figs. 1(d) and (e)). Possible optimal measurement frames for the  $m = 4, 6, 8, 12$  and 20 cases are thus defined by the vertices of the Platonic solids inscribed in the Poincaré sphere, in agreement with the numerical results of [20]. The inscribed polyhedra generated for  $m = 4, 6$  and 12 correspond to the polyhedra of maximal volume. In contrast, however, noting that inscribed polyhedra of maximal volume are Euclidean simplexes [36], i.e. each face is triangular, the cube and dodecahedron do not have maximum volume in contrast to the claim of [20]. Non-uniqueness of the solution to Eq. (4) implies the associated polyhedra for

arbitrary  $m$  are also not of maximal volume in general.

**Odd  $m$ :** When  $m$  is a factorable odd integer the ansatz used thus far is also capable of generating optimal measurement frames. In Fig. 1(h), for example, a possible optimal frame is shown for  $(m, r, s) = (9, 3, 3)$ , with  $\cos \theta_2 = 0$  and  $\cos \theta_{1,3} = \pm 1/\sqrt{2}$ . For prime  $m$  alternative solutions must, however, be sought. It is well known that no spherical 2-design, and hence no optimal frame, exists for  $m = 5$  [34], as can be verified by calculation of the Groebner basis [37] of the set of polynomial equations given by Eqs. (4) and the constraints  $\mathbf{a}_j^T \cdot \mathbf{a}_j = 1$ . Solutions for larger prime  $m$  can nevertheless still be found. One such solution set (also valid for factorable odd  $m$ ) takes the form  $\mathbf{a}_j = (\sin \theta_j \cos \phi_j, \sin \theta_j \sin \phi_j, \cos \theta_j)$ , where  $\phi_j = 2\pi j/(m-1)$ ,  $\cos \theta_j = c_1$  for  $j = 1, 3, \dots, m-2$ ,  $\cos \theta_j = c_2$  for  $j = 2, 4, \dots, m-1$ ,  $\cos \theta_m = 1$  and  $c_i = [3 \pm (-1)^i \sqrt{3m(m-4)}]/[3(1-m)]$  as follows from Eq. (4). This solution is depicted in Figs. 1(i)-(k) for  $m = 7, 9$  and 11.

The underlying mathematical framework found above hints at a potential extension of the optimisation procedure to higher order measurement problems. Consider, for example, the measurement of a nonlinear function  $D(\mathbf{S})$ , such as the generated intensity in an optical nonlinear conversion problem. Letting  $P_k(\mathbf{S})$  denote a complete basis of polynomial functions, ordered by increasing polynomial degree and indexed by  $k = 0, 1, \dots, \infty$ , the measurand can be decomposed according to

$$D(\mathbf{S}) = \sum_{k=0}^{\infty} F_k P_k(\mathbf{S}) \quad (6)$$

where  $F_k$  are the associated expansion coefficients which are now the unknowns of interest.  $P_k$  are assumed to be orthonormal over the Poincaré sphere. Practically, a finite number of measurements,  $m$ , are made in directions  $\{\mathbf{A}_j\}$  so as to sample  $D(\mathbf{S})$ . Furthermore, the sum in Eq. (6) must be truncated at a finite order  $K$ , such that Eq. (6) reduces to  $\mathbf{D} = \mathbb{P} \mathbf{F}$ , where  $\mathbf{F} = (F_0, F_1, \dots, F_K)^T$  and  $[\mathbb{P}]_{jk} = P_k(\mathbf{A}_j)$ . In general, at least  $K+1$  measurements are required for complete determination of  $\mathbf{F}$ . Optimality in this case can again be quantified using the condition number of  $\mathbb{P}$ . Assuming the polynomials  $P_k$  satisfy  $\sum_{k=0}^K P_k^*(\mathbf{S}) P_k(\mathbf{S}) = C$ , where  $C$  is a constant, a trace constraint analogous to Eq. (1) follows. Noting  $P_0(\mathbf{S})$  is also a constant, similar derivations to above yield

$$\kappa^2 = \frac{C}{P_0} + \frac{CK^2}{C - P_0^2}, \quad (7)$$

where the corresponding optimal Gram matrix  $\mathbb{P}^\dagger \mathbb{P}$  must be diagonal. The resulting constraints (c.f. Eq. (4)) are satisfied if the analysis states constitute a spherical  $2t$ -design, where  $t$  is the degree of the polynomial  $P_K$ . Proof follows in a similar fashion to above. As a concrete example, if the polynomial functions  $P_k$  are taken

as the spherical harmonics  $Y_{lm}$  (whereby the  $k$  index in Eq. (6) denotes a suitable lexicographic ordering of the indices  $(l, m)$ ) up to maximum degree  $l = t$ , it follows that  $K = (t+1)^2$  and  $P_0 = 1/\sqrt{4\pi}$ . Using the addition theorem  $\sum_{m=-l}^l Y_{lm}^* Y_{lm} = (2l+1)/(4\pi)$  the minimum achievable condition number is found to be  $\kappa = (t+1)^2$ . Importantly, it should be noted that spherical  $2t$  designs do not necessarily exist for arbitrary  $m$  [35]. In general it is therefore found that estimation of higher order properties not only becomes more ill-conditioned, but also requires a larger number of measurements to be made. Use of optimal measurement sets is therefore critical to reconstruction quality in this case. In this sense the Platonic solids perform well as measurement frames since they constitute higher order  $t$ -designs, e.g. a regular dodecahedron is a spherical 5-design, whilst possessing a relatively small number of analysis states.

In summary, optimal measurement frames for the reconstruction of the Stokes vector  $\mathbf{S}$  of polarised light have been analytically and geometrically investigated. This analysis can also be applied to the input polarisation states in Mueller matrix polarimetry [38]. Equivalence of optimisation based on the EWV, the condition number  $\kappa$  of the associated instrument matrix and the determinant of its Gram matrix was established. Constraints on the optimal analysis states were derived and found to be satisfied by states defining spherical 2-designs. It followed that minimisation of  $\kappa$  does not necessarily correspond to maximisation of the volume of the corresponding inscribed polyhedron. Finally, results were extended to consider optimal frames when the measurand is a polynomial function of  $\mathbf{S}$  of degree  $t$ . In this case optimal frames correspond to sets of analysis states constituting spherical  $2t$  designs. This work provides the means for optimal polarisation state tomography and hence paves the way for practical study of nonlinear or stochastic properties of polarisation, which are of interest in both biological and physical contexts. Within the former, for example, nonlinear polarisation studies can provide insight into cellular and molecular structure [23, 39], whilst the latter can enable study of fundamental quantum polarisation properties [28, 40, 41]. Finally, these results also present interesting opportunities for establishing optimal schemes for quantum tomography of two level systems due to the underlying geometric parallels with the Bloch sphere.

The authors acknowledge Markus Grassl for suggesting the connection between the linear problem and spherical 2-designs and for Luis L. Sánchez-Soto and Gerd Leuchs for insightful discussions. AF acknowledges financial support from the Gordon and Betty Moore Foundation.

---

\* [matthew.foreman@mpl.mpg.de](mailto:matthew.foreman@mpl.mpg.de)

[1] J. Z. Salvail, M. Agnew, A. S. Johnson, E. Bolduc,

- J. Leach, and R. W. Boyd, “Full characterization of polarization states of light via direct measurement,” *Nat. Photon.* **7**, 316–321 (2013).
- [2] E. Hadamcik, A. K. Sen, A. C. Levasseur-Regourd, R. Gupta, and J. Lasue, “Polarimetric observations of comet 67P/Churyumov-Gerasimenko during its 2008–2009 apparition,” *Astron. Astrophys.* **517**, A86 (2010).
- [3] D. Sofikitis, L. Bougas, G. E. Katsoprinakis, A. K. Spiliotis, B. Loppinet, and T. P. Rakitzis, “Evanescent-wave and ambient chiral sensing by signal-reversing cavity ringdown polarimetry,” *Nature* **514**, 76–79 (2014).
- [4] M. R. Foreman, C. Macías-Romero, and P. Török, “Determination of the three dimensional orientation of single molecules,” *Opt. Lett.* **33**, 1020–1022 (2008).
- [5] J. N. Damask, *Polarization Optics in Telecommunications*, Springer Series in Optical Sciences (Springer-Verlag, New York, New York, 2005).
- [6] D. S. Sabatke, M. R. Descour, E. L. Dereniak, W. C. Sweatt, S. A. Kemme, and G. S. Phipps, “Optimization of retardance for a complete Stokes polarimeter,” *Opt. Lett.* **25**, 802–804 (2000).
- [7] F. Goudail, “Noise minimization and equalization for Stokes polarimeters in the presence of signal-dependent Poisson shot noise,” *Opt. Lett.* **34**, 647–649 (2009).
- [8] M. R. Foreman, C. Macías-Romero, and P. Török, “A priori information and optimisation in polarimetry,” *Opt. Express* **16**, 15212–15227 (2008).
- [9] M. R. Foreman and P. Török, “Information and resolution in electromagnetic optical systems,” *Phys. Rev. A* **82**, 043835 (2010).
- [10] J. S. Tyo, “Optimum linear combination strategy for an N channel polarization sensitive imaging or vision system,” *J. Opt. Soc. Am. A* **15**, 359–366 (1998).
- [11] A. S. Alenin, *Matrix Structure for Information Driven Polarimeter Design* PhD Thesis (University of Arizona, 2015).
- [12] R. M. A. Azzam, “Optimal beam splitters for the division-of-amplitude photopolarimeter,” *J. Opt. Soc. Am.* **20**, 955–958 (2003).
- [13] A. Ambirajan and D. C. Look, “Optimum angles for a polarimeter: part I,” *Opt. Eng.* **34**, 1651–1655 (1995).
- [14] A. Ambirajan and D. C. Look, “Optimum angles for a polarimeter: part II,” *Opt. Eng.* **34**, 1656–1658 (1995).
- [15] J. S. Tyo, “Design of optimal polarimeters: maximization of signal-to-noise ratio and minimization of systematic error,” *Appl. Opt.* **41**, 619–630 (2002).
- [16] R. M. A. Azzam, I. M. Elminyawi, and A. M. El-Saba, “General analysis and optimization of the four-detector photopolarimeter,” *J. Opt. Soc. Am. A* **5**, 681–689 (1988).
- [17] S. N. Savenkov, “Optimisation and structuring of the instrument matrix for polarimetric measurements,” *Opt. Eng.* **41**, 965–972 (2002).
- [18] M. H. Smith, “Optimization of a dual-rotating-retarder Mueller matrix polarimeter,” *Appl. Opt.* **41**, 2488–2493 (2002).
- [19] K. M. Twietmeyer and R. A. Chipman, “Optimization of Mueller matrix polarimeters in the presence of error sources,” *Opt. Express* **16**, 11589–11603 (2008).
- [20] A. Peinado, A. Lizana, J. Vidal, C. Iemmi, and J. Campos, “Optimization and performance criteria of a Stokes polarimeter based on two variable retarders,” *Opt. Express* **18**, 9815–9830 (2010).
- [21] A. Aiello, G. Puentes, D. Voigt, and J. P. Woerdman, “Maximum-likelihood estimation of Mueller matrices,” *Opt. Lett.* **31**, 817–819 (2006).
- [22] Y. Shi, W. M. McClain, and R. A. Harris, “Generalized Stokes Mueller formalism for two photo absorption, frequency doubling and hyper Raman scattering,” *Phys. Rev. A* **49**, 1999–2015 (1994).
- [23] M. Samim, S. Krouglov, and V. Barzda, “Double Stokes Mueller polarimetry of second-harmonic generation in ordered molecular structures,” *J. Opt. Soc. Am. B* **32**, 451–461 (2015).
- [24] R. Barakat, “Statistics of the Stokes parameters,” *J. Opt. Soc. Am. A* **4**, 1256–1263 (1987).
- [25] A. Aiello and J. Woerdman, “Physical bounds to the entropy-depolarization relation in random light scattering,” *Phys. Rev. Lett.* **94**, 090406 (2005).
- [26] J. J. Gil, “Polarimetric characterization of light and media : physical quantities involved in polarimetric phenomena,” *Eur. Phys. J. Appl. Phys.* **47**, 1–47 (2007).
- [27] P. De La Hoz, A. B. Klimov, G. Björk, Y. H. Kim, C. Müller, C. Marquardt, G. Leuchs, and L. L. Sánchez-Soto, “Multipolar hierarchy of efficient quantum polarization measures,” *Phys. Rev. A* **88**, 063803 (2013).
- [28] J. Söderholm, G. Björk, A. B. Klimov, L. L. Sánchez-Soto, and G. Leuchs, “Quantum polarization characterization and tomography,” *New. J. Phys.* **14** (2012).
- [29] V. V. Prasolov, *Problems and theorems in linear algebra*, vol. 134 of *Translations of Mathematical Monographs* (American Mathematical Society, Providence, RI, 1994).
- [30] P. Roman, “Generalized stokes parameters for waves with arbitrary form,” *Il Nuovo Cimento* **13**, 974–982 (1959).
- [31] D. Haase and H. Stachel, “Almost-orthonormal vector systems,” *Beitr. Algebra Geom.* **37**, 367–381 (1996).
- [32] A. Klappenecker and M. Rötteler, “Mutually unbiased bases are complex projective 2-designs,” arXiv:quantph/0502031 (2005).
- [33] P. Delsarte, J. M. Goethals, and J. J. Seidel, “Spherical codes and designs,” *Geometriae Dedicata* **6**, 363–388 (1977).
- [34] Y. Mimura, “A construction of spherical 2-design,” *Graphs Combi.* **6**, 369–372 (1990).
- [35] R. H. Hardin and N. J. A. Sloane, “McLaren’s improved snub cube and other new spherical designs in three dimensions,” *Discrete Comput. Geom.* **15**, 429–441 (1996).
- [36] J. D. Berman and K. Hanes, “Volumes of polyhedra inscribed in the unit sphere in E3,” *Math. Ann.* **188**, 78–84 (1970).
- [37] D. Cox, J. Little, and D. O’Shea, *Ideals, varieties, and algorithms* (Springer-Verlag, Berlin, 2007).
- [38] D. Layden, M. F. G. Wood, and I. A. Vitkin, “Optimum selection of input polarization states in determining the sample Mueller matrix: a dual photoelastic polarimeter approach,” *Opt. Express* **20**, 20466–20481 (2012).
- [39] N. Mazumder, J. Qiu, M. R. Foreman, C. M. Romero, C.-W. Hu, H.-R. Tsai, P. Török, and F.-J. Kao, “Polarization-resolved second harmonic generation microscopy with a four-channel Stokes polarimeter,” *Opt. Express* **20**, 14090–14099 (2012).
- [40] A. B. Klimov, G. Björk, J. Söderholm, L. Madsen, M. Lassen, U. Andersen, J. Heersink, R. Dong, C. Marquardt, G. Leuchs, and L. L. Sánchez-Soto, “Assessing the Polarization of a Quantum Field from Stokes Fluctuations,” *Phys. Rev. Lett.* **105**, 153602 (2010).
- [41] A. Holleczek, A. Aiello, C. Gabriel, C. Marquardt, and G. Leuchs, “Classical and quantum properties of cylin-

drically polarized states of light.” *Opt. Express* **19**, 9714–9736 (2011).